Discover Applied Sciences

Research

In vitro evaluation and characterization of cisplatin loaded nanofibers for local chemotherapy

Carlos Miguel López Mendoza[1] · Yolanda Terán Figueroa[2] · Mariana Gutiérrez Sánchez[3] · María Mónica Castillo Ortega[4] · Nayeli Rodríguez Fuentes[5] · Luz Eugenia Alcántara Quintana[6]

Received: 20 April 2023 / Accepted: 20 November 2023
Published online: 18 March 2024

Abstract
Cancer is a disease that affects the quality of life of the patients that are treated with Cisplatin (CDDP), which is needed for adjuvant therapy, however it leads to many secondary and adverse effects. In this study, we manufactured and characterized poly-(lactic acid) (PLA) non-woven fibers loaded with Cisplatin (CDDP) by electrospinning technique to evaluate their cytotoxicity in in vitro assays on HeLa cells (cervical carcinoma cell line). PLA–CDDP solutions with increasing concentrations of CDDP (0.5, 1 and 2% w/w) were used in a TL-01 electrospinning equipment with the same system parameters. We analyzed the chemical, thermal and morphological characteristics of PLA and PLA–CDDP fiber mats. Furthermore, hydrolytic degradation, hemolysis and toxicity in HeLa cells were evaluated. By adding the CDDP to the fibers, the degradation, glass transition and melting temperatures were modified; the 3 µm fiber diameter of pristine PLA fibers was decreased in half the size and the degradation time was extended over 5 months. However, the hemocompatibility of the material with and without CDDP was maintained, while cytotoxicity in HeLa cells increased in the three concentrations of fiber mats of PLA–CDDP compared to the intravenous drug at 24 h ($p < 0.01$). We concluded that the fiber mats PLA–CDDP could be used for localized therapy in the adjuvant treatment when resection panels are expose after a surgical extirpation of solid tumors.

Highlights

- Cisplatin loaded polymer fiber meshes were developed by electrospinning.
- Drug loaded fibers induced toxicity in cervical cancer cell line in vitro.
- Electrospun fibers can be an alternative localized therapy.

✉ Luz Eugenia Alcántara Quintana, lealcantara@conacyt.mx; luz.alcantara@uaslp.mx | [1]Autonomous University of San Luis Potosí, San Luis Potosí, Mexico. [2]Faculty of Nursing and Nutrition, Autonomous University of San Luis Potosí, San Luis Potosí, Mexico. [3]Faculty of Stomatology, Autonomous University of San Luis Potosí, San Luis Potosí, Mexico. [4]Department of Research in Polymers and Materials, University of Sonora, Hermosillo, Mexico. [5]Biomaterials Unit, CONACYT Chair, Yucatan Scientific Research Center, Mérida, Mexico. [6]Coordination for Innovation and Application of Science and Technology, CONACYT Chair, Autonomous University of San Luis Potosí, Sierra Leona 5550, Lomas 2a Sección, 78120 San Luis Potosí, México.

Graphical Abstract

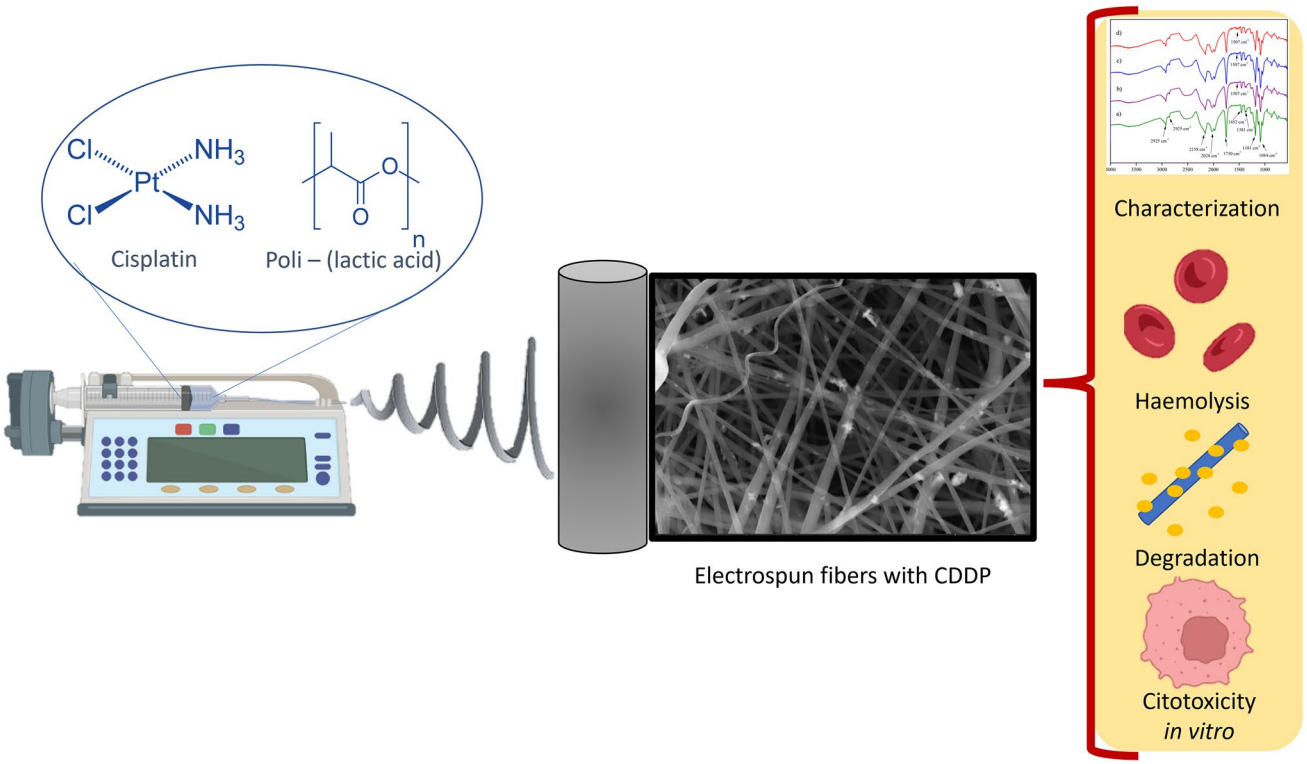

Keywords Poly-(lactic acid) · Cisplatin · Electrospinning · HeLa · Cancer

1 Introduction

Cancer is a disease caused by uncontrolled cell growth and division in a tissue, and it can appear anywhere in the body [1]. It is the sixth leading cause of death around the world with 18 million new cases only in 2018. In Mexico in the same year, the cases increased to 190,600, with a projected increase in the next 20 years [2–4].

Chemotherapy is part of the treatment regimen to combat this disease in order to shrink the tumor or eliminate metastatic cells in the system (neoadjuvant or adjuvant therapy) [5–7]. Cisplatin (CDDP), one of the drugs used in these therapies, is characterized by being a chelating antineoplastic agent, recommended as an adjuvant in metastatic lung, liver, or stomach cancer, although it is also used for cervical and head-neck cancer [8, 9].

Cisplatin exerts its activity upon entering the cell, and its mechanism of action is based on acting as an electrophilic molecule, being able to bind to thiol groups of enzymes and structural proteins in addition to forming adducts in the DNA, thus causing cellular death [10]. The application of intravenous chemotherapy leads to a whole-body distribution by blood, hence adverse effects appear, such as nausea, vomiting, anemia, toxicity in vital organs and long-term sequelae in the patient's life. [11–16], in addition to the fact that cells can generate resistance to these drugs [17–19]. That is why, one of the challenges of chemotherapy is to reduce systemic toxicity, and one way to approach this end is using Drug Delivery Systems (DDS).

For example, Zong et al. [20] obtained fibers from PLA and poly (ethylene oxide) (PEO) by electrospinning, encapsulating CDDP within the fibers, which was then tested in a murine model. The efficacy of the DDS loaded with CDDP was evaluated by weighting of the tumor in the cervix after the days of treatment, additionally other organs were extracted for the quantification of CDDP. The in-situ treatments with fibers charged with CDDP and the drug administered by IV route, at the same doses, were compared. The tumors weighed the same after the treatments, with the difference that

the therapy with the charged fibers decreased the amount of CDDP in organs such as kidneys, heart and liver, and high concentrations were found in the tumor and peritumoral area. The opposite happened with the IV treatment, demonstrating the safety of the fibers in situ.

In vivo models indicates that the local therapy of cancer solid tumors or in resection margins, have a potential over the intravenous treatment, with two advantages over the systemic treatment, that are, (1) efficacy and (2) safety to major organs. Additionally, nanofibers as local drug delivery, have exhibit sustained release in in vitro and in vivo models, increasing drug concentration in the site of action, with the advantages of suppression of generalized toxicity, higher efficacy in diminishing tumor volume or cancer cells in the resection margins. DDS have also shown that due to their immediate and recurrent action in the place where they should exert their activity, they can prevent cells from acquiring resistance to antineoplastic drugs, avoiding therapeutic failure [21–24].

There are several ways to design a fiber-based DDS, which can be through template-assisted synthesis techniques, self-assembly, solvent casting, phase separation and electrospinning, the latter being the most widely used for providing greater surface area due the small diameter of the fibers and for ease of use. In the electrospinning process, polymeric solutions are used, made from synthetic polymers, biopolymers, or copolymers, for the creation of fibers conjugated to drugs, genes, nanoparticles, excitatory molecules by physical means, among others. [25–29]. This method is influenced by the process conditions, the concentrations and characteristics of the polymers used [30, 31]. Additionally, electrospun fiber meshes are the target for works that involve tissue regeneration, drug delivery, other platforms encapsulation with the advantages of tunable nanofibers depending on the challenges to overcome [32, 33].

Biodegradable polymers are currently used in these processes due to their degradation and their compatibility with the human body [34–36]. Poly (lactic acid) (PLA) is one of the most widely used materials, for example, in implants, orthopedic equipment and tissue engineering, because it degrades by hydrolysis, which then, the L-lactic acid monomers are absorbed by cells and used in the Krebs cycle until they are eliminated as CO_2 and H_2O. Furthermore, it has been observed in medical devices, based on PLA, that it does not generate immunogenicity when inside the body [37–40].

Thus, the objective of the present work is to manufacture poly (lactic acid) (PLA) fibers charged with different concentrations of Cisplatin (CDDP) by electrospinning technique, to characterize their morphological, chemical, and thermal properties and to evaluate their cytotoxicity in in vitro tests with HeLa cervical cancer cells.

2 Materials and methods

2.1 Materials

Poly (L-lactic acid) (PLA) in 3D printing filament and Cisplatin (CDDP) obtained from Sigma Aldrich, chloroform (JT BAKER) and N,N dimethylformamide (DMF, Biopack) were used. Dubelcco's PBS technique with individual salts and then the sterilization process, Saline 0.9% (Pisa), Triton X-100 (Sigma Aldrich). A cervical cancer cell line, HeLa ATCC CCL-2, was used for cytotoxic evaluation, Dulbecco0s Modified Eagle Medium (DMEM, Gibco), Fetal Bovine Serum (FBS, Gibco), Penicillin–Streptomycin (Sigma Aldrich) and 3-(4,5-Dimethyl-2-thiazolyl)-2,5-diphenyl-2H-tetrazolium Bromide (MTT, Merck).

2.2 System parameters

Firstly, 1.67 g of PLA was deposited into a beaker with cap, then a mixture of 8 mL of Chloroform (CHCl3) and 2 mL of N,N dimethylformamide (DMF) was poured with the polymer and letting blend overnight at room temperature, with a final concentration of 8% wt/wt of PLA. For the loaded polymer solution, 8.28 mg, 16.56 mg, and 22.09 mg of CDDP were poured into different beakers with cap, with the addition of 2 mL of DMF in each one, putting in constant stirring for 6 h. In other beaker, a solution of PLA 8% wt/wt was prepared. The CDDP-DMF and PLA 8% wt/wt solutions were blended and stirred constantly for 12 h, to obtain 3 different solutions of PLA–CDDP with different concentration of CDDP, 0.5% wt/wt, 1% wt/wt and 2% wt/wt based on PLA weight.

2.3 Electrospinning process

The polymers solutions with pristine PLA and PLA loaded with 0.5, 1 and 2% wt/wt were added to a 20 mL syringe, which was then used in the TL-01 electrospinning apparatus from Tong Li Tech. The conditions used were modified from those

obtained by Gutiérrez et al. [41] due to the addition of DMF and CDDP. A volume of 6 mL was used; flow rate of 3 mL/h; rotating collector plate moving speed of 200 rpm; axial speed of 2 mm/s; 7-Gauge needle and the distance between the tip of the needle and the collector roll was 15 cm.

2.4 Characterization

A Thermo Scientific Nicolet 1510 ATR-Diamond kit was used to obtain the infrared spectra of fiber mat samples. The spectra were obtained by ATR mode using a resolution of 4 with 64 scans in the spectral range between 400–4000 cm^{-1}. For thermal characterization, Differential Scanning Calorimetry (DSC) was used with a DSC Q2000 equipment from TA Instruments Inc., in which 10 mg of sample was encapsulated and subjected to two heating cycles at 5 °C/min from − 10 to 180 °C under N_2 atmosphere. The crystallinity assessment results were obtained by de equation of degree of crystallinity:

$$\Delta Xc = \frac{\Delta H_{sample}}{\Delta H_m^0}$$

where, ΔHsample stands for the valor of melting enthalpy and $\Delta H^0{}_m$ is the enthalpy of melting for a fully crystallized PLLA sample (93.1 J/g). Likewise, Thermogravimetric Analysis (TGA) was performed using a Perkin Elmer TGA 8000 equipment. In this process, a 7 mg sample was subjected to a heating rate from 50 to 650 °C with a rate of 10 °C/min under an atmosphere of N_2.

2.4.1 Morphology

Electrospun fibers were observed using Scanning Electron Microscopy (SEM) in a Helios G4CX equipment at a voltage of 30 kV. Previously, the meshes were coated with gold by means of cathodic assisted sputtering. The micrographs were used to measure a total of 100 fibers per sample and the average of these were analysed using ImageJ software (National Institutes of Health, USA).

2.4.2 Degradation test

Samples of 1 cm^2 were weighed and placed in conical tubes with 5 mL of sterile Phosphate Buffer Saline (PBS) (pH 7.44) and left in constant stirring at 37 °C for a period of 0, 1, 3 and 5 months, with PBS change every week. The weight loss of the entire fiber meshes was measured. Final products of degradation and molecular weight changes were not assessed [42].

2.4.3 Hemolysis test

A 1:50 solution of erythrocytes and sterile PBS (pH 7.2) was obtained. Then, 1 cm^2 samples of the fibers were prepared and allowed to soak for 30 min in PBS, prior to contact with erythrocytes. Subsequently, they were added to the solution for 1 h with constant stirring. They were then centrifuged at 5000 ×*g* for 5 min and the absorbance at 541 nm was read. The percentage of hemolysis obtained with the following equation was reported:

$$\%Hemolysis = \frac{sample\ absorbance - negative\ absorbance}{positive\ absorbance - negative\ absorbance} X100$$

The absorbance value of the positive and negative controls and of the sample [43].

2.5 Assays in cell culture

The HeLa cervical cancer cell line was used. The cells were cultured in DMEM medium, supplemented with 10% inactivated fetal bovine serum (FBS) and 1% penicillin/streptomycin (AB). They were incubated at 37 °C in an atmosphere of 95% air, 5% CO_2 and 98% humidity.

2.5.1 Cell viability study

We follow the instructions of ISO 10993-5; Biological evaluation of medical devices—Part 5: Tests for in vitro cytotoxicity. HeLa cells were cultured in a 96-well microculture plate, at a concentration of 5×10^5 cells/well in DMEM/10% Serum fetal bovine/1% antibiotic medium, incubated for 24 h at 37 ± 0.5 °C. We divided the plate into five groups, (1) Positive control, cells with CDDP; (2) the fibers as P0Pt for PLA pristine fiber meshes, like negative control; (3) P1Pt, (4) P2Pt and (5) P3Pt correspond to added drug, 0.5, 1 and 2% (wt /wt) of CDDP loaded in the fiber meshes. The percent growth inhibition was measured using MTT [3-(4,5-dimethylthiazol-2-yl)-2,5-diphenyltratazolium bromide], which is a colorimetric assay of metabolic activity as indicator of viability. The reduction of MTT (yellow) by metabolic active cells to formazan crystals (purple), then we measure the absorbance of formazan at 570 nm [44]. The percentage of viability is calculated with the following equation:

$$\%Viability = \frac{average\ sample\ (OD\ 570e\ nm)}{average\ blanks\ (OD\ 570b\ nm)} \times 100$$

where. OD570e is the mean value of the measured optical density of the 100% of the sample; and OD570b is the mean value of the measured optical density of the blanks.

2.6 Statistical analysis

Data are expressed as arithmetic mean with standard deviation. Statistical analysis was performed using ANOVA analysis with Dunett's multiple comparison post hoc test, the level of significance was defined as $p < 0.05$. The analyzes were performed using the GraphPad Prism program (version 6 for Microsoft Windows). The statistical analysis used for cell viability assay was an ANOVA test with post hoc of Dunnet's, with $n = 5$ for every sample, the comparisons are made to evaluate the differences between the cytotoxicity level that was produced by the cisplatin release from the fibers, the alpha level in this test was 95% one tail and the P valor of 0.05.

3 Results

The loaded polymer solution changed the color from white (PLA only) to a light yellow. Solutions were stable during the electrospinning process. There was also a change in process parameters, in flow rate and voltage used, from 2 to 3 mL/h and 8 kV to 9 kV in order to prevent solvent evaporation in the spinneret. We obtained 4 fiber mats with area of 460 cm^2 with different concentrations of CDD. For practical purposes we named the fibers as P0Pt for PLA pristine fiber meshes; P1Pt, P2Pt and P3Pt correspond to added drug, 0.5, 1 and 2% (wt/wt) of CDDP loaded in the fiber meshes.

3.1 FTIR

We analyzed the infrared spectra together of the P0Pt to P3Pt fibers (Fig. 1a), which share characteristic bands at 2150 and 1750 cm^{-1} associated with the ester bonds of PLA. However, those fibers with CDDP showed an increase in bands in the areas of 1640–1560 cm^{-1}, and one special band in 1507 cm^{-1} (Fig. 1b), which are associated with bonds of the amino groups of CDDP, demonstrating the presence of the pharmacological agent [45–47].

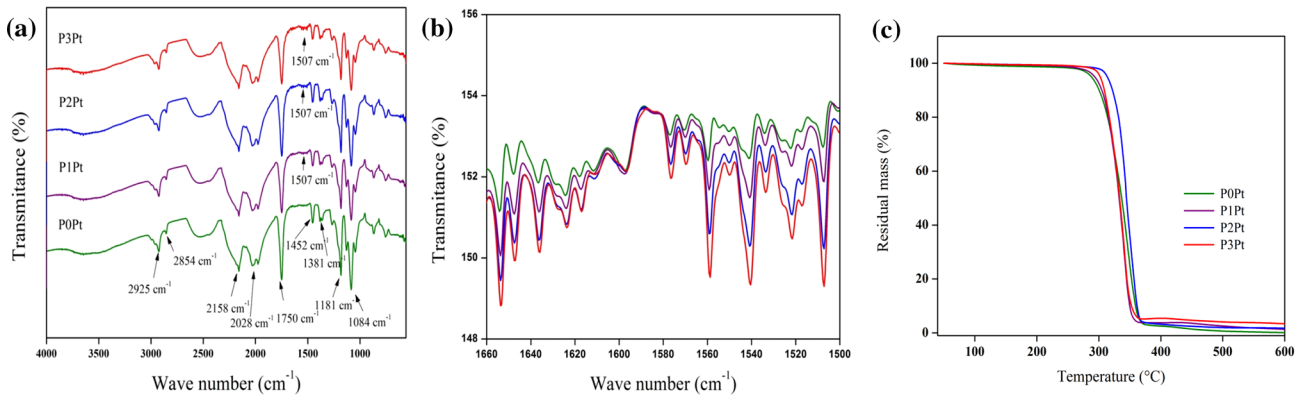

Fig. 1 The infrared spectra of the P0Pt to P3Pt fibers and Thermogram of the fibers. **a** FT-IR spectra of the fibers. Which share characteristic bands at 2150 and 1750 cm^{-1} associated with the ester bonds of PLA. **b** Enlargement of the area of 1660–1500 cm^{-1}. Are associated with bonds of the amino groups of CDDP. Transmitance (%), Wave number (cm^{-1}). **C** Thermal behavior was also evaluated using the TGA technique. A weight loss of 97% is observed for the P0Pt sample from 280 °C, culminating at up to 400° C. Residual mass (%), Temperature (°C)

Table 1 DSC curves of the second heating cycle

Sample	Tg (°C)	Tc (°C)	Tm (°C)	Hc (J/g)	Hm (J/g)	ΔXc (%)
P0Pt	60.0	115.0	148.1	5.9	5.0	5.4
P1Pt	58.9	112.4	147.1	4.7	3.8	4.0
P2Pt	59.0	112.8	147.1	3.5	2.8	2.9
P3Pt	60.0	114.0	147.3	4.2	3.8	4.0

Characteristic temperatures of the fibers

Tg Glass transition temperature, *Tc* crystallization temperature, *Tm* melting temperature, *Hc* enthalpy of crystallization, *Hm* enthalpy of fusion

3.2 DSC

Using the DSC curves of the second heating cycle, the characteristic temperatures of semi-crystalline materials were obtained (Table 1), where variations in temperatures and enthalpies associated with the alteration in PLA chains due to the incorporation of CDDP can be observed but these modifications are not associated with chemical bonding of Cisplatin—PLA. However, the degree of crystallinity decreased from the PLA pristine fiber meshes, when CDDP is added, but no in a significant manner, because the fraction of crystallinity in four samples of fiber meshes were ~ 5%, indicating we have been managing a semicrystalline polymer, according to the DSC characteristic profile.

3.3 TGA

The thermal behavior was also evaluated using the TGA technique (Fig. 1c), where a weight loss of 97% is observed for the P0Pt sample at 280 °C, culminating in near 0% mass at up to 400 °C. These results are similar to the temperatures reported by Qiu K. et al. [27]. On the other hand, P0Pt fibers (Tmax = 350 °C) had greater thermal stability than those containing CDDP (P1Pt Tmax = 341 °C; P2Pt Tmax = 343 °C; P3Pt Tmax = 341 °C). Also, the latter presented residual mass percentages at 600 °C (P1Pt = 1.3%; P2Pt = 1.7%; P3Pt = 3.39%) which can be attributed to the platinum content in the samples, since this metal has its point melting above 1400 °C, and for the same reason, no other loss event is seen [48]. The residual mass is above the theory weight (0.5, 1 and 2%) due a failure in the system parameters, not a fully homogenization of the polymeric solution with cisplatin could make some of the fibers had a greater amount in different zones.

3.4 Morphology

In the micrographs (Fig. 2a, c, e, g) we can see that the fibers are randomly arranged and have a smooth surface. In addition, in the P3Pt, an agglomerate of CDDP is observed outside its surface but contained within the composite. This

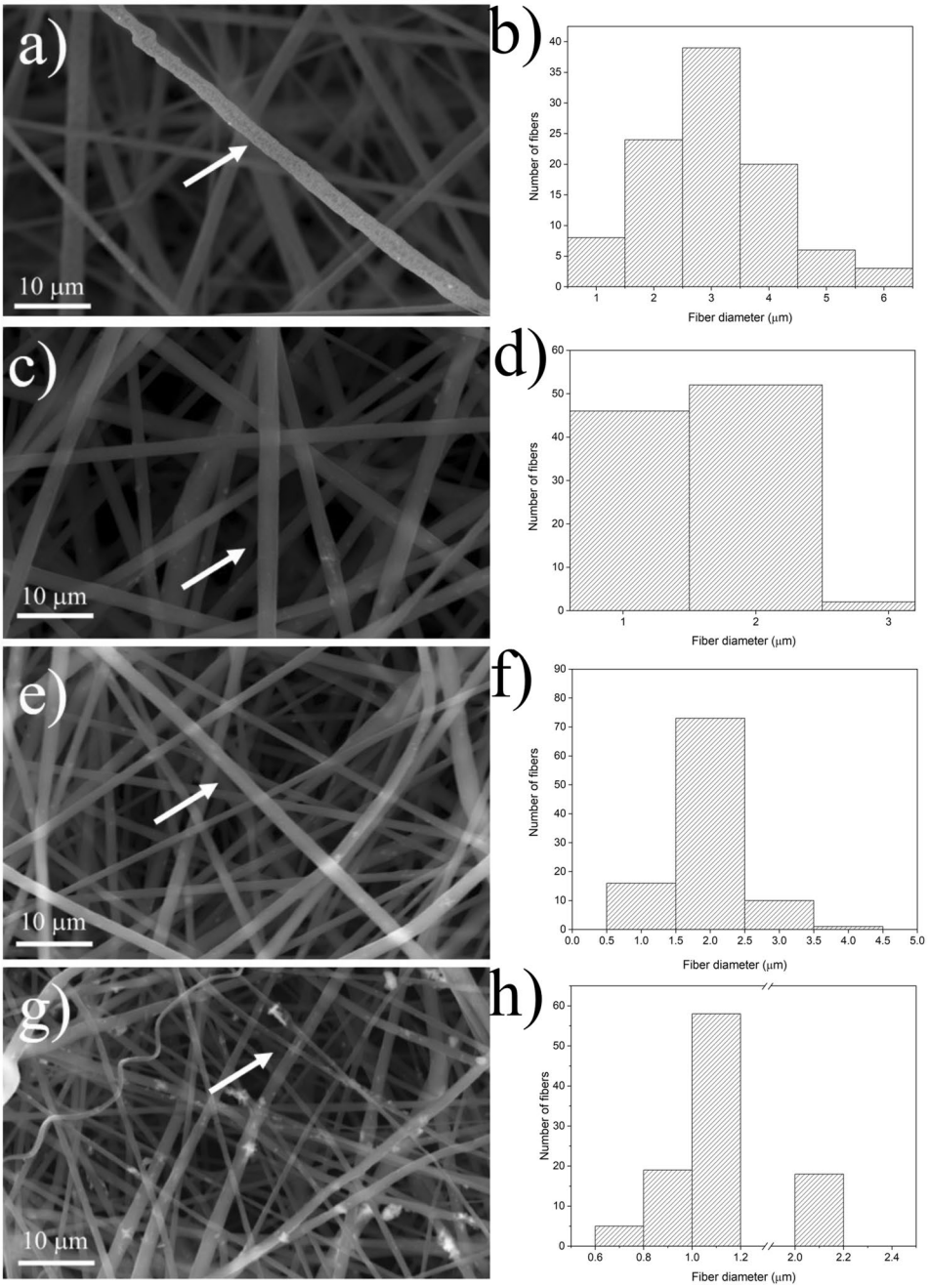

Fig. 2 Morphology assay: Micrographs with their respective fiber diameter histograms: **a** and **b** P0Pt; **c** and **d** P1Pt; **e** and **f** P2Pt; **g** and **h** P3Pt

may be due the polymer solution with which they were made was based on supersaturated DMF, therefore, only a part CDDP was solubilized [46]. The agglomerates only were present in loaded nanofibers; for P1Pt nanofibers we found 11 in each micrograph with a mean size of 0.53 µm, P2Pt agglomerates mean size were 0.76 µm with a frequency of 22 per micrograph and P3Pt with a frequency of 38 per micrograph mean size were 1.68 µm. Likewise, we observed that when the drug was added to the fibers, they decreased their size (Fig. 2b, d, f, h) from P0Pt with a diameter mean size of 2980 nm ± 1091 nm; P1Pt with 1557 nm ± 541 nm; P2Pt with 2140 nm ± 1885 nm to P3Pt with 1150 nm ± 405 nm. This is attributable to the platinum contained in the solution, since it has been shown to affect the surface charge of the solution, increasing the repulsive force of the magnetic field under the applied voltage, causing the jet of expelled polymer to thin. Consequently, we obtained fibers of less diameter than the P0Pt [49–51]. The statistical analysis used for this assay was a mean with standard deviation (SD), with n = 10 for every sample, no statistical comparisons were made.

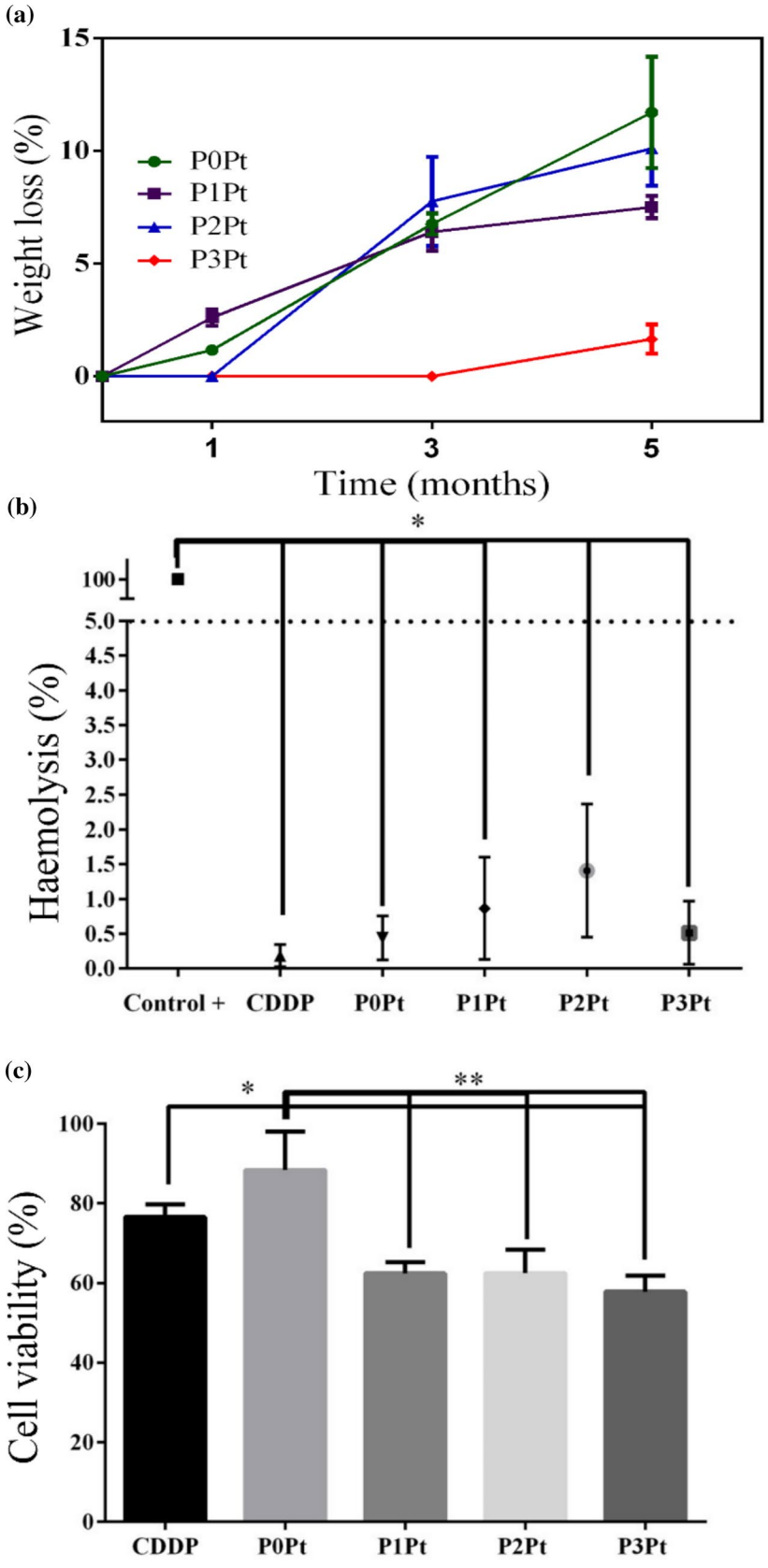

Fig. 3 Degradation assay, Hemocompatibility test, and In vitro cytotoxicity: **A** degradation assay. Frequency (%), Fiber diameter (µm or mm). (a) Fiber weight loss, there was no change in weight or shape in the first three months and (b) pH decrease of the medium over time. Weight loss (%), Time (months). **B** Hemocompatibility graph, we observed that CDDP does not exert a damaging effect on the erythrocyte membrane in the time of 1 h, and the same happened for fibers with and without drug*. **C** Cell viability test, determined by the MTT assay. The P3Pt fibers decreased cell viability by approximately 40% since, in addition to having a greater amount of encapsulated CDDP**. *P < 0.05, **P < 0.01. Hemolysis (%), Cell viability (%)

3.5 Degradation assay

The degradation of the nanofiber meshes were assessed via mass loss (Fig. 3a). Hydrolytic degradation in this type of composites occurs in two ways, homogeneous and heterogeneous. In the homogeneous one, the area of the fibers does not change, but it swells and releases what is inside the composite. On the other hand, heterogeneous way, where surface erosion and deformation of the fibers are observed [52]. However, fibers meshes were not assessed for CDDP release or homogeneity of degradation. Therefore, we observed mass loss of the material, although it is well known that PLA does not degrade quickly but can maintain its initial weight in in vitro tests up to 6 months [53]. The mass changes and characterization at the end of the periods of evaluation exceed the aim of this manuscript is a perspective for a future work.

3.6 Hemolysis test

In this test (Fig. 3b), we observed that CDDP does not exert a damaging effect on the erythrocyte membrane in the time of 1 h, and the same happened for fibers with and without drug ($p < 0.05$), which is similar to that observed by Da Silva et al. [54] where they evaluated PLA particles, and these were below the limit of 5% of allowance of the American Society of Testing and Materials (ASTM) [54]. The statistical analysis used for this assay was an ANOVA test with post hoc of multiple comparisons, with $n = 9$ for every sample, the comparisons are made to evaluate the differences among the samples with and without CDDP, the alpha level in this test was 95% one tail and the P valor of 0.05.

3.7 In vitro cytotoxicity

We obtained the percentage of cell viability by means of an MTT assay (Fig. 3c). The HeLa cells were put in contact with the different fibers and the free cisplatin for 24 h. For practical purposes we named the fibers as P0Pt for PLA pristine fiber meshes; P1Pt, P2Pt and P3Pt correspond to added drug, 0.5, 1 and 2% (wt/wt) of CDDP loaded in the fiber meshes. Subsequently, cell viability was determined. The P3Pt fibers decreased cell viability by approximately 40%, in addition to having a greater amount of encapsulated CDDP, they presented agglomerates of drug outside the fiber, resulting in what is known as burst release, which is the release of the drug directly to the medium without degradation of the fibers, to later enter a constant release stage. Furthermore, the diameter has an influence, since, as has been observed, the larger the diameter of the drug-containing fibers, the greater the impediment for its release, since the surface must first be broken. Therefore, the P1Pt and P2Pt fibers had less effect than the P3Pt [55]. The P3Pt fibers had a significant difference ($p < 0.05$) when compared the cytotoxicity to the free drug control, so we could assert that in the in vitro trials, the fiber treatment works, although studies are needed to determine if it works as a treatment in situ in an in vivo model.

The importance of cancer therapy radicates in the challenge of completely cure a patient without reducing their life quality more, therefore surgery of solid tumors is a standard and needs to be conjugated with other therapies because of the cancer recurrence. Chemotherapy can be used in adjuvant or neoadjuvant ways, adjuvant comes before tumor resection, the advantages of using a localized therapy can improve the concentration in situ and systemic safety vs i.v. injection of cisplatin [20]. Although, adjuvant chemotherapy is given after tumor resection because of the recurrence of tumor and circulating tumor cells; locally implanted cisplatin loaded nanofibers have diminished the tumor recurrence rate in a 100% with a survival rate of 60% in 45 days, in contrast to cisplatin i.v. which had an inhibition rate of 80% with a survival rate of 0% after the same time period with a notable reduction in weight of the test subjects, meaning systemic damage [56]. Hence, loaded nanofibers are a promising alternative for localized tumor therapy.

4 Conclusions

Electrospun fiber meshes have diverse opportunities in the field of scaffolds or local drug delivery due their improvement of properties over other polymeric strategies. Cytotoxic fiber meshes were successfully made in our study, decreasing the viability of HeLa cells (cervical cancer), in contrast of free dug treatment in vitro, and having a nonhemolytic profile. Further analysis needs to be made, to make out of this cytotoxic meshes a strategy for local chemotherapy in an early state of solid tumors or resection margins with the insight of increasing patient's life quality and decreasing systemic effects.

Acknowledgements This research was supported by the National Council of Science and Technology (CONACYT) with the grant number 929186.

Author contributions CMLM, data curation, formal analysis, investigation process, validation, redaction; YTF, resources, supervision; MGS, methodology, supervision, validation; MMCO, supervision, methodology; NRF, supervision, methodology; LEAQ, conceptualization, methodology, project administration, resources, supervision, redaction.

Funding This study was funded by Consejo Nacional de Ciencia y Tecnología, 929186.

Data and code availability Data available on request from authors.

Declarations

Ethics approval and consent to participate No ethical approval was required for this research as it did not involve human tissue or other parts of living organisms.

Competing interests The authors declare that they have no competing interests.

References

1. Hyndman IJ. Review: the contribution of both nature and nurture to carcinogenesis and progression in solid tumours. Cancer Microenviron. 2016;9:63–9. https://doi.org/10.1007/s12307-016-0183-4.
2. World Health Organization. Top 10 causes of death. 2018. https://www.who.int/gho/mortality_burden_disease/causes_death/top_10/en/> Accessed 15 June 2019.
3. World Health Organization. Cancer Country Profile 2020. Mexico Burden of Cancer World Heal. Organ. 2020. pp. 2019–20.
4. INEGI. Estadísticas a propósito del día Mundial contra el Cáncer de Mama, Infocancer Mex. 2018. pp. 1–13. http://www.infocancer.org.mx/?c=cancer-cifras&a=estadisticas-2018. Accessed 10 Jun 2022.
5. Schirrmacher V. From chemotherapy to biological therapy: a review of novel concepts to reduce the side effects of systemic cancer treatment (review). Int J Oncol. 2019. https://doi.org/10.3892/ijo.2018.4661.
6. Oh JJ. Adjuvant chemotherapy. Amsterdam: Elsevier Inc.; 2018. https://doi.org/10.1016/B978-0-12-809939-1.00026-6.
7. O'Halloran N, Lowery A, Curran C, McLaughlin R, Malone C, Sweeney K, Keane M, Kerin M. A Review of the impact of neoadjuvant chemotherapy on breast surgery practice and outcomes. Clin Breast Cancer. 2019;19:377–82. https://doi.org/10.1016/j.clbc.2019.04.011.
8. Aldossary SA. Review on pharmacology of cisplatin: clinical use, toxicity and mechanism of resistance of cisplatin. Biomed Pharmacol J. 2019;12:7–15. https://doi.org/10.13005/bpj/1608.
9. Pendleton KP, Grandis JR. Cisplatin-based chemotherapy options for recurrent and/or metastatic squamous cell cancer of the head and neck. Clin Med Insights Ther. 2013;5:103–16. https://doi.org/10.4137/CMT.S10409.
10. Shaloam D, Tchounwou PB. Cisplatin in cancer therapy: molecular mechanisms of action. Eur J Pharmacol. 2014;740:364–78. https://doi.org/10.1016/j.ejphar.2014.07.025.Cisplatin.
11. Barabas K, Milner R, Lurie D, Adin C. Cisplatin: a review of toxicities and therapeutic applications. Vet Comp Oncol. 2008;6:1–18.
12. Zanto TP, Hennigan K, Östberg M, Clapp WC, Gazzaley A. Predictive knowledge of stimulus relevance does not influence top-down suppression of irrelevant information in older adults. Cortex. 2011;46:564–74. https://doi.org/10.1016/j.cortex.2009.08.003.Predictive.
13. Volarevic V, Djokovic B, Jankovic MG, Harrell CR, Fellabaum C, Djonov V, Arsenijevic N. Molecular mechanisms of cisplatin-induced nephrotoxicity: a balance on the knife edge between renoprotection and tumor toxicity. J Biomed Sci. 2019;9:1–14.
14. Bryer E. Chemotherapy-induced anemia: etiology, pathophysiology, and implications for contemporary practice. Int J Clin Trans Med. 2018. https://doi.org/10.2147/IJCTM.S187569.
15. El-awady EE, Moustafa YM, Abo-elmatty DM, Radwan A. Cisplatin-induced cardiotoxicity: mechanisms and cardioprotective strategies. Eur J Pharmacol. 2011;650:335–41. https://doi.org/10.1016/j.ejphar.2010.09.085.
16. Nurgali K, Jagoe RT, Abalo R. Editorial: adverse effects of cancer chemotherapy: anything new to improve tolerance and reduce sequelae? Front Pharmacol. 2018;9:1–3. https://doi.org/10.3389/fphar.2018.00245.
17 Mansoori B, Mohammadi A, Davudian S, Shirjang S, Baradaran B. The different mechanisms of cancer drug resistance: a brief review. Med Sci. 2017;7:339–48. https://doi.org/10.15171/apb.2017.041.
18. Rebucci M, Michiels C. Molecular aspects of cancer cell resistance to chemotherapy. Biochem Pharmacol. 2013;85:1219–26. https://doi.org/10.1016/j.bcp.2013.02.017.
19. Shen D, Pouliot LM, Hall MD, Gottesman MM. Cisplatin resistance: a cellular self-defense mechanism resulting from multiple epigenetic and genetic. Changes. 2012;64:706–21.

20. Zong S, Wang X, Yang Y, Wu W, Li H, Ma Y, Lin W, Sun T, Huang Y, Xie Z, Yue Y, Liu S, Jing X. The use of cisplatin-loaded mucoadhesive nanofibers for local chemotherapy of cervical cancers in mice. Eur J Pharm Biopharm. 2015;93:127–35. https://doi.org/10.1016/j.ejpb.2015.03.029.
21. Poláková L, Širc J, Hobzová R, Cocârță AI, Heřmánková E. Electrospun nanofibers for local anticancer therapy: review of in vivo activity. Int J Pharm. 2019;558:268–83. https://doi.org/10.1016/j.ijpharm.2018.12.059.
22 Senapati S. Controlled drug delivery vehicles for cancer treatment and their performance. Sig Transduct Target Ther. 2018. https://doi.org/10.1038/s41392-017-0004-3.
23. Zhong G, Yang C, Liu S, Zheng Y, Lou W, Teo JY, Bao C, Cheng W, Tan JPK, Gao S, Park N, Venkataraman S, Huang Y, Tan MH, Wang X, Hedrick JL, Fan W, Yang YY. Polymers with distinctive anticancer mechanism that kills MDR cancer cells and inhibits tumor metastasis. Biomaterials. 2019;199:76–87. https://doi.org/10.1016/j.biomaterials.2019.01.036.
24. Fu Y, Li X, Ren Z, Mao C, Han G. Multifunctional electrospun nanofibers for enhancing localized cancer treatment. Small. 2018;1801183:1–21. https://doi.org/10.1002/smll.201801183.
25 Torres EJ, Cornejo JM, Medina AS, Pérez GL, Villareal LJ. A summary of electrospun nanofibers as drug delivery system: drugs loaded and biopolymers used as matrices. Curr Drug Deliv. 2018. https://doi.org/10.2174/1567201815666180723114326.
26. Gherasim O, Grumezescu A, Grumezescu V, Iordache F, Vasile B, Holban A. Bioactive sufaces of polylactide and silver nanoparticles for the prevention of microbal contamination. Mat. 2020;13:1–15. https://doi.org/10.3390/ma13030768.
27. Qiu K, He C, Feng W, Wang W, Zhou X, Yin Z, Chen L, Wang H, Mo X. Doxorubicin-loaded electrospun poly(l-lactic acid)/mesoporous silica nanoparticles composite nanofibers for potential postsurgical cancer treatment. J Mater Chem B. 2013;1:4601–11. https://doi.org/10.1039/c3tb20636j.
28 Lee S, Jin G, Jang J. Electrospun nanofibers as versatile interfaces for efficient gene delivery. J Biol Eng. 2014;8:1–19.
29. Zhang Z, Liu S, Xiong H, Jing X, Xie Z, Chen X, Huang Y. Electrospun PLA/MWCNTs composite nanofibers for combined chemo- and photothermal therapy. ACTA Biomater. 2015. https://doi.org/10.1016/j.actbio.2015.08.003.
30 Haider A, Haider S, Kang I. A comprehensive review summarizing the effect of electrospinning parameters and potential applications of nanofibers in biomedical and biotechnology. Arab J Chem. 2018;11:1165–88. https://doi.org/10.1016/j.arabjc.2015.11.015.
31. Kumar A, Sinha-Ray S. A review on biopolymer-based fibers via electrospinning and solution blowing and their applications. Fibers. 2018;6:1–53. https://doi.org/10.3390/fib6030045.
32. Mousavi SM, Nejad ZM, Hashemi SA, Salari M, Gholami A, Ramakrishna S, Chiang WH, Lai CW. Bioactive agent-loaded electrospun nanofiber membranes for accelerating healing process: a review. Membranes. 2021;11(9):702. https://doi.org/10.3390/membranes11090702.
33. Roseti L, Parisi V, Petretta M, Cavallo C, Desando G, Bartolotti I, Grigolo B. Scaffolds for bone tissue engineering: state of the art and new perspectives. Mater Sci Eng C. 2017;78:1246–62. https://doi.org/10.1016/j.msec.2017.05.017.
34. Jacob J, Haponiuk JT, Thomas S, Gopi S. Biopolymer based nanomaterials in drug delivery systems: a review. Mater Today Chem. 2018;9:43–55. https://doi.org/10.1016/j.mtchem.2018.05.002.
35. Rebelo R, Fernandes M, Fangueiro R. Biopolymers in medical implants: a brief review. Procedia Eng. 2017;200:236–43. https://doi.org/10.1016/j.proeng.2017.07.034.
36. Vroman I, Tighzert L. Biodegradable polymers. Materials. 2009;2:307–44. https://doi.org/10.3390/ma2020307.
37. Singhvi MS, Zinjarde SS, Gokhale DV. Polylactic acid: synthesis and biomedical applications. J Appl Microbiol. 2019;127:1612–26. https://doi.org/10.1111/jam.14290.
38. Gregor A, Filová E, Novák M, Kronek J, Chlup H, Buzgo M, Blahnová V, Lukášová V, Bartoš M, Nečas A, Hošek J. Designing of PLA scaffolds for bone tissue replacement fabricated by ordinary commercial 3D printer. J Biol Eng. 2017;11:1–21. https://doi.org/10.1186/s13036-017-0074-3.
39. Tyler B, Gullotti D, Mangraviti A, Utsuki T, Brem H. Polylactic acid (PLA) controlled delivery carriers for biomedical applications. Adv Drug Deliv Rev. 2016;107:163–75. https://doi.org/10.1016/j.addr.2016.06.018.
40. da Silva D, Kaduri M, Poley M, Adir O, Krinsky N, Shainsky-Roitman J, Schroeder A. Biocompatibility, biodegradation and excretion of polylactic acid (PLA) in medical implants and theranostic systems. Chem Eng J. 2018;340:9–14. https://doi.org/10.1016/j.cej.2018.01.010.
41. Gutiérrez-Sánchez M, Escobar-Barrios VA, Pozos-Guillén A, Escobar-García DM. RGD-functionalization of PLA/starch scaffolds obtained by electrospinning and evaluated in vitro for potential bone regeneration. Mater Sci Eng C. 2019;96:798–806. https://doi.org/10.1016/j.msec.2018.12.003.
42. International Organization for Standardization. Occupational health and safety management systems—requirements with guidance for use (ISO/DIS Standard No. 10993). 2016. http://www.iso.org/iso/catalogue_detail?csnumber=63787. Accessed 15 Sep 2022.
43. Shitole AA, Raut PW, Sharma N, Giram P, Khandwekar AP, Garnaik B. Electrospun polycaprolactone/hydroxyapatite/ZnO nanofibers as potential biomaterials for bone tissue regeneration. J Mater Sci Mater Med. 2019;30(5):51. https://doi.org/10.1007/s10856-019-6255-5.
44. Mahmoudifard M, Soleimani M, Hatamie S, Zamanlui S, Ranjbarvan P, Vossoughi M, Hosseinzadeh S. The different fate of satellite cells on conductive composite electrospun nanofibers with graphene and graphene oxide nanosheets. Biomed Mater. 2016;11(2):025006. https://doi.org/10.1088/1748-6041/11/2/025006.
45. Auras R, Lim LT, Selke SEM, Tsuji H. Poly (lactic acid): synthesis, structures, properties, processing, and applications. Hoboken: John Wiley and Sons; 2010. https://doi.org/10.1002/9780470649848.
46. Vhora I, Khatri N, Desai J, Thakkar HP. Caprylate-conjugated cisplatin for the development of novel liposomal formulation. AAPS PharmSciTech. 2014;15:845–57. https://doi.org/10.1208/s12249-014-0106-y.
47 Xiao X, Wang T, Li L, Zhu Z, Zhang W, Cui G. Co-delivery of cisplatin (IV) and capecitabine as an effective and non-toxic cancer treatment. Front Pharmacol. 2019;10:1–9. https://doi.org/10.3389/fphar.2019.00110.
48 Tseng C-L, Yang K-C, Yen K-C, Yueh-Hsiu Wu S, Lin F-H. Preparation and characterization of cisplatin-incorporated Gelatin nanocomplex for cancer treatment. Curr Nanosci. 2011;7:932–37. https://doi.org/10.2174/157341311798220736.
49. Absar S, Khan M, Edwards K, Calamas D (2014) Electrospinning of cisplatin-loaded cellulose nanofibers for cancer drug delivery

50. Aggarwal U, Goyal AK, Rath G. Development and characterization of the cisplatin loaded nanofibers for the treatment of cervical cancer. Mater Sci Eng C. 2017;75:125–32. https://doi.org/10.1016/j.msec.2017.02.013.
51. Chen P, Wu QS, Ding YP, Zhu ZC. Preparation of cisplatin composite micro/nanofibers and antitumor activity in vitro against human tumor spc-a-1 cells. NANO. 2011;6:325–32. https://doi.org/10.1142/S1793292011002688.
52. Elsawy MA, Kim KH, Park JW, Deep A. Hydrolytic degradation of polylactic acid (PLA) and its composites. Renew Sustain Energy Rev. 2017;79:1346–52. https://doi.org/10.1016/j.rser.2017.05.143.
53 Da Silva J, Jesus S, Bernardi N, Colaço M, Borges O. Poly (D, L-lactic acid) nanoparticle size reduction increases its immunotoxicity. Front Bioeng Biotechnol. 2019;7:1–10. https://doi.org/10.3389/fbioe.2019.00137.
54. ASTM E2524-08. Standard test method for analysis of hemolytic properties of nanoparticles. West Conshohocke: ASTM International; 2013.
55. Chen SC, Huang XB, Cai XM, Lu J, Yuan J, Shen J. The influence of fiber diameter of electrospun poly(lactic acid) on drug delivery. Fibers Polym. 2012;13:1120–5. https://doi.org/10.1007/s12221-012-1120-x.
56. Zhang Y, Liu S, Wang X, et al. Prevention of local liver cancer recurrence after surgery using multilayered cisplatin-loaded polylactide electrospun nanofibers. Chin J Polym Sci. 2014;32:1111–8. https://doi.org/10.1007/s10118-014-1491-0.